RSC Sustainability

ROYAL SOCIETY OF CHEMISTRY

PAPER

View Article Online
View Journal | View Issue

Cite this: *RSC Sustainability*, 2025, **3**, 3198

Microbial degradation of tannery chrome-solid waste using *Bacillus thuringiensis*: optimization of collagen hydrolysate extraction *via* response surface methodology†

Sharmin Akter Liza and Md. Abdulla-Al-Mamun *

A significant amount of chrome-containing shaving dust is generated by the leather industry during leather processing, posing a threat to both the ecosystem and human health. Its widespread disposal, including the mixing of leachate with groundwater, leads to a decline in water quality, while incineration can convert Cr(III) into the carcinogenic Cr(VI). Since shaving dust contains a substantial amount of protein, discarding it without recovering this valuable resource would be a considerable waste, as it could be repurposed to produce various profitable goods such as protein hydrolysate. This study presents an efficient and eco-friendly approach for managing chrome shaving dust through microbial degradation using the *Bacillus thuringiensis* strain SRL4A (PP802975). The bacterium exhibited optimal growth after 36 hours of incubation at 45 °C, at pH 8, and demonstrated high chromium resistance, tolerating up to 900 ppm of Cr(III) salts. Response Surface Methodology (RSM) was employed in conjunction with Central Composite Design (CCD) to investigate the impact of independent variables (seed volume, nutrient source, and time) on the response variable degradation. The optimum values of the independent process parameters for maximum degradation (94.80%) were obtained at 35% (v/w) seed volume, 12.86% (w/w) nutrient source, and 101.27 hours of incubation time. Analysis of Variance (ANOVA) confirmed that the degradation of chrome shavings was primarily influenced by seed volume, followed by nutrient source and time. Hydrolysates were collected at various intervals during proteolysis, chromium was removed, and the samples were characterized. The final protein and chromium content in the hydrolysate were 979.44 ± 4.88 mg L^{-1} and 1.40 ± 0.37 mg L^{-1}, respectively. UV-vis and FTIR spectroscopy analysis demonstrated characteristic protein peaks. TGA indicated the higher thermal stability of the recovered collagen hydrolysate. SEM revealed a porous protein sample, and EDX confirmed the presence of C, N, O, and S elements. The findings of this research provide valuable insights into developing sustainable strategies for managing tannery waste per principles of circular economy and environmental stewardship.

Received 25th October 2024
Accepted 4th June 2025

DOI: 10.1039/d4su00666f

rsc.li/rscsus

Sustainability spotlight

A significant amount of chrome-containing shaving dust is generated by the leather industry during leather processing, posing a threat to both the ecosystem and human health. Its widespread disposal, including the mixing of leachate with groundwater, leads to a decline in water quality, while incineration can convert Cr(III) into the carcinogenic Cr(VI). Since shaving dust contains a substantial amount of protein, discarding it without recovering this valuable resource would be a considerable waste, as it could be repurposed to produce various profitable goods such as protein hydrolysate. It was reported that chromium-cross-linked collagen has a higher protein content of 75–79% and 4.4% chromic oxide. It also makes up 15–30% of the total amount of protein waste tanneries create. Due to the presence of chromium, these disposal methods are increasingly posing substantial concerns and harming the ecosystem. Disposal in low-lying regions without adequate liners results in the mixing of leachate with groundwater, leading to a decline in water quality. Approximately 40–50% of methane gas is released from uncontrolled landfills of shaving dust, significantly contributing to the climate crisis. Additionally, this chromium seeps into the ground, rendering it unsuitable for cultivation and many other purposes, while the incineration process can convert Cr(III) to Cr(VI). Previous research focused on obtaining collagen and chromium using different chemical agents and sometimes enzymes, inferring this to deal with solid waste management systems. The chemicals employed in the process are not environmentally friendly, and additional stages are occasionally required to extract these materials. This makes the procedures complex, time-consuming, and expensive. Moreover, enzyme accelerated procedures generate significant chrome sludge that requires additional large-scale treatment. However, most of these previous studies have focused on the impact of individual experimental parameters, as it is time-consuming, laborious, and complicated to execute the vast number of experiments necessary to ascertain their combined effects. Therefore, several statistical analogies have been employed in recent years to optimize processes and investigate parameter interaction in a significantly reduced number of experiments, thereby reducing the cost and time required. To fill

Institute of Leather Engineering and Technology, University of Dhaka, 44-50 Hazaribagh, Dhaka 1209, Bangladesh. E-mail: mamun.ilet@du.ac.bd

† Electronic supplementary information (ESI) available. See DOI: https://doi.org/10.1039/d4su00666f

these knowledge and experimental gaps, we employed a comprehensive approach that included the isolation of chrome-tolerant bacteria, targeted protein quantification, and a process designed to be efficient, time-saving, and cost-effective. Response Surface Methodology (RSM) is one of the most frequently implemented tools for process optimization. This study presents an efficient and eco-friendly approach for managing chrome shaving dust through microbial degradation using the *Bacillus thuringiensis* strain SRL4A (PP802975). The bacterium exhibited optimal growth after 36 hours of incubation at 45 °C, at pH 8, and demonstrated high chromium resistance, tolerating up to 900 ppm of Cr(III) salts. Response Surface Methodology (RSM) was employed in conjunction with Central Composite Design (CCD) to investigate the impact of independent variables (seed volume, nutrient source, and time) on the response variable degradation. The optimum values of the independent process parameters for maximum degradation (94.80%) were obtained at 35% (v/v) seed volume, 12.86% (w/w) nutrient source, and 101.27 hours of incubation time. Analysis of Variance (ANOVA) confirmed that the degradation of chrome shavings was primarily influenced by seed volume, followed by nutrient source and time. Hydrolysates were collected at various intervals during proteolysis, chromium was removed, and the samples were characterized. The final protein and chromium content in the hydrolysate were 979.44 ± 4.88 mg L^{-1} and 1.40 ± 0.37 mg L^{-1}, respectively. UV-vis and FTIR spectroscopy were demonstrated, and found the characteristic protein peaks. TGA indicated the higher thermal stability of the recovered collagen hydrolysate. SEM revealed a porous protein sample, and EDX confirmed the presence of C, N, O, and S elements. The findings of this research provide valuable insights into developing sustainable strategies for managing tannery waste per principles of circular economy and environmental stewardship.

1 Introduction

The use of chromium(III) salts is currently the most popular technique for tanning, with almost 90% of the world's leather produced by chrome tanning.[1,2] A significant amount of chrome-containing waste is generated during the production of leather. One metric ton of raw hide/skin is estimated to yield 200 kg of leather, 200 kg of tanned waste, 250 kg of non-tanned waste, and 50 m^3 of wastewater.[3] Among the solid waste, chrome shaving dust is one of the most notable tanned wastes. These tiny shaving dust particles are generated through a mechanical shaving process, which is carried out to attain the required thickness of the leather. It has been reported that chromium-cross-linked collagen has a higher protein content of 75–79% and 4.4% chromic oxide.[4] It also makes up 15–30% of the total amount of protein waste tanneries create.[5]

In most developing countries, including Bangladesh, most of this shaving dust is disposed of through on-site open burning and landfilling. Due to the presence of chromium, these disposal methods are increasingly posing substantial concerns and harming the ecosystem. Disposal in low-lying regions without adequate liners results in the mixing of leachate with groundwater, leading to a decline in water quality. Approximately 40–50% of methane gas is released from uncontrolled landfills of shaving dust, significantly contributing to the climate crisis.[6,7] Additionally, this chromium seeps into the ground, rendering it unsuitable for cultivation and many other purposes, while the incineration process can convert Cr(III) to Cr(VI).[6] Furthermore, these methods of disposal are costly and ineffectual. Due to the abovementioned problems, stringent restrictions on the leather industry worldwide have prompted research into re-utilizing waste to generate wealth. Since shaving dust contains a significant amount of protein, dumping it without recovering this protein would also be a substantial waste of a resource that could be utilized to produce various profitable goods. Additionally, the escalation of disposal costs, challenges in locating suitable landfill areas, and the upsurge in protein costs have led to increased emphasis on the reutilization of chrome shavings.[8]

Therefore, current technological methodologies for recycling these collagen by-products have focused on the extraction and isolation of collagen/protein hydrolysate and chromium from leather shavings *via* a hydrolysis process utilizing chemicals, enzymes, and acidic or alkaline environments.[9–12] Shanthi *et al.*, (2013) utilized a potent, chromium-tolerant bacterium identified as *Alcaligenes faecalis*, which degraded 90% of shaving dust in just 5 days when administered in the optimal dosage.[13] Katsifas *et al.*, (2004) used *Aspergillus carbonarius* to study the degradation of chrome shavings in solid-state fermentation, achieving liquefaction of the tannery waste to the extent of around 97% in a long-term experiment.[14]

Previous research focused on obtaining collagen and chromium using different chemical agents and sometimes enzymes, inferring this to deal with solid waste management systems. The chemicals employed in the process are not environmentally friendly, and additional stages are occasionally required to extract these materials. This makes the procedures complex, time-consuming, and expensive. Moreover, enzyme accelerated procedures generate significant chrome sludge that requires additional large-scale treatment. However, most of these previous studies have focused on the impact of individual experimental parameters, as it is time-consuming, laborious, and complicated to execute the vast number of experiments necessary to ascertain their combined effects. Therefore, several statistical analogies have been employed in recent years to optimize processes and investigate parameter interaction in a significantly reduced number of experiments, thereby reducing the cost and time required. To fill these knowledge and experimental gaps, we employed a comprehensive approach that included the isolation of chrome-tolerant bacteria, targeted protein quantification, and a process designed to be efficient, time-saving, and cost-effective. Response Surface Methodology (RSM) is one of the most frequently implemented tools for process optimization. It is a mathematical approach extensively employed to optimize processes and identify the influencing parameters.[15] RSM predicts the impact of process parameters by analyzing individual and cumulative interactions to determine an optimal range.[16] It enhances the reproducibility of results and the efficiency of processes. The statistical design of experiments can also aid in selecting optimal conditions and processes, producing more reliable information than conventional methods.

The present study explored the applicability and usefulness of employing a chrome-tolerant bacterium, *Bacillus thuringiensis* SRL4A, isolated from soil to extract collagen and chromium from shaving dust through degradation. Microorganism-assisted degradation is a cleaner process because it breaks down

complex substances into smaller intermediates without any negative impact on the surrounding environment.[17,18] Degradation by microbes alone could be a more cost-effective, less complex, and environmentally friendly method, as it entails minimal use of harmful chemicals. The degradation process was able to convert waste into valuable wealth successfully. The collagen hydrolysate can be used as peptones, packaging material, bio stimulators, scaffolds, soil conditioners/fertilizers, cosmetics, building materials, biodegradable polymers, poultry and animal feed, glue, leather finishes, edible gelatin, and as a filler in the retanning stage of leather processing.[19] The residual chrome precipitate can be used to make different colored pigments for the ceramics industry.[20] The experimental parameters and their interactions, such as seed volume, nutrient source, and time, were optimized using the Central Composite Design (CCD) feature of Response Surface Methodology (RSM), as is the case in industrial-scale fermentation processes, where the cost of the nutrient medium and enhancement of enzyme production are vital considerations.[21]

To the best of our knowledge, this is the first time that such an isolation method, optimization process, and application for tannery chrome-containing solid waste have been reported. To fill this gap in the existing literature, this study has two primary objectives. Firstly, it seeks to enhance knowledge about the specific bacterial isolation process for chrome shaving dust degradation and the optimization of bacterial activity. In particular, the research aims to provide a more comprehensive understanding of the key stakeholders in the value chain, their primary strategies for valorizing tannery shaving waste and extracting collagen, with the most influential related socio-economic factors. This study offers a valuable opportunity to improve practical applications and advance the understanding of circular models and metrics that are relevant and useful to organizations in the tannery sector.

2 Materials and method

2.1 Chemicals and materials

Tryptone (pancreatic digest of casein) and Bovine Serum Albumin (BSA) were obtained from Sigma-Aldrich. Skim milk agar, nutrient broth media, and nutrient agar media were obtained from HiMedia Laboratories Pvt. Ltd. API® 50CH panel (50 CHB/E medium) and were collected from BioMérieux. Purified NaOH pellets, hydrochloric acid (37%), have been supplied by Active Fine Chemicals Ltd., Dhaka, Bangladesh. Acetone, methanol, phosphoric acid and nitric acid, and ethanol were procured from Merck KGaA, Darmstadt, Germany. All samples' solutions were prepared using purified distilled water from a UV water purification system purchased from Labtron Equipment Ltd., UK. All chemicals and reagents were utilized without further purification.

2.2 Soil sampling and collection

The soil was obtained from the front side of the Institute of Leather Engineering and Technology, University of Dhaka (23.73° N, 90.37° E). The sample was collected in large quantities from the top layer (0–15 cm deep), gathered in aseptic plastic containers, and stored at 4 °C until needed.

2.3 Isolation of bacteria

The serial dilution method was used to isolate and count the microorganisms. One gram of the collected soil was added to the first falcon tube and serially diluted up to a 10^{-6} dilution, with the 10^{-5} dilution being employed in subsequent analyses. Skim milk agar media was prepared and autoclaved at 15 lbs pressure and 121 °C for 15 minutes for sterilization. The bacterial consortium was grown using the spread plating technique, which involved introducing 0.1 mL from the 10^{-5} diluted sample and spreading it with an L-rod until it was completely absorbed into the media. The Petri dishes were then incubated at 37 °C and monitored for microbial development for 48 hours. To isolate a pure colony using the streak plate method, a colony with the largest clearance zone and similar bacteria was chosen after 48 hours. Nutrient agar media was prepared and sterilized, and then streaked with each pure colony using the quadrant streaking technique. The Petri dishes were incubated at 37 °C for 48 hours and observed for a pure isolated colony.

2.4 Screening of a proteolytic bacterial isolate for protease production

2.4.1 Primary screening. On the same skimmed milk agar media plate, the isolate was first screened by spot inoculation using a sterile platinum wire loop, and the plate was then incubated at 37 °C. Due to proteolytic activity, a clearing zone was observed surrounding the inoculation site.

2.4.2 Secondary screening. Selected isolates from primary screening were then grown in a nutrient broth medium at pH 7. This is known as the bacterial pre-culture or seed. Then, 1% of the fully grown culture was inoculated in a freshly prepared nutrient broth and incubated at 37 °C at 150 rpm in a rotary shaker. The culture was centrifuged at 7000 rpm for 20 minutes at 4 °C. The enzyme solutions were taken to determine protease activity.

2.5 Determination of proteolytic activity

The protease activity of the strain was measured using the universal protease test that uses casein as a substrate. The tyrosine standard curve was also obtained to measure the protease activity. The absorbance for both methods was measured with a UV-vis spectroscopy at 680 nm.[22] Here, one unit of proteolytic activity denotes to the amount of enzyme that releases 1 μg tyrosine per mL per minute. The activity (U/mL) of the enzyme was determined using eqn (1):

$$(U/\mathrm{mL}) = \frac{\mu\mathrm{M\ of\ tyrosine} \times \mathrm{total\ volume\ of\ assay(mL)}}{\mathrm{time\ of\ the\ assay(minutes)} \times \mathrm{amount\ of\ enzyme(mL)} \times \mathrm{volume\ used\ in\ spectrophotometer(mL)}} \quad (1)$$

2.6 Morphological characterization of bacteria

2.6.1 Gram staining. A 24 hour-old culture was prepared, smeared on a slide, and then fixed with heat. Then, after being treated with crystal violet for 1 minute, the smear was rinsed with distilled water. It was then flooded with a solution of gram iodine for 1 minute and then rinsed it with an alcohol solution. Finally, it was overrun with safranin, washed with distilled water, dried, and observed under oil immersion.[23]

2.6.2 Motility test. The motility test was done using an MIU medium base that is generally used to determine motility, indole, and urea-producing bacteria through one examination. 1.89% of the media was added to distilled water, dissolved by heating, and transferred to 3–4 mL per test tube. The tubes were sterilized by autoclaving and cooled to 50–60 °C. Then, with a sterilized platinum wire loop, fresh bacterial culture was carefully inoculated by keeping the platinum wire loop in a vertical position up to two-thirds of the semi-solid media. The tubes were then incubated at 37 °C for 24–48 hours.

2.6.3 Endospore staining. This staining was done by fixing the smear with heat on a microscopic slide. Malachite green (0.5 g per 100 mL of water) was used to show the endospore. The slide was covered with a paper cut to match the size of the slide, and malachite green was flooded on the slide dropwise. Care was taken so that the stain did not dry. It was kept on the hot beaker for 5 minutes. Then, the stain was rinsed with water. Safranin was then added and rinsed away. It was observed under an electronic microscope.[24]

2.7 Biochemical characterizations of bacteria

The bacterial isolate was initially identified using API (Analytical Profile Index). It is a system that categorizes bacteria by performing biochemical tests, enabling quick identification. API test strips feature wells with dehydrated substrates that detect enzymatic activity, usually associated with the introduced organisms' breakdown of proteins and amino acids or fermentation of carbohydrates. 50 CH and 20 E strips were used to determine the bacterium. The bacterium colony was suspended in 0.85% NaCl for the API 20 E strip and 50 CH B medium for the API 50 CH strip to match the McFarland standard 2. The suspension was used to rehydrate each well of the first 12 wells of the 20 E strip and the wells of the 50 CH strip, excluding the cupules. The remaining 8 wells of API 20 E strips were not rehydrated as these tests are replicated on the API 50 CH strip. The strips were kept in an incubator and examined for any color changes. The API 50 CH test was conducted to identify Bacillus species. The initial 12 tests of the API 20 E strip were conducted with the API 50 CH strip test for additional testing.

These supplemental tests are not required for Bacillus and its related taxa but are essential for Enterobacteriaceae and Vibrionaceae. Carbohydrates underwent fermentation to produce acids, leading to a pH fall, as shown by a color change in the indicator. These findings form the biochemical profile, which the identification program analyses to recognize the strain.

2.8 DNA extraction and 16S rRNA gene identification

The genomic DNA of the isolate was extracted using a Bacterial Genomic DNA extraction kit according to the manufacturer protocol (QIAGEN, QIAamp DNA Mini Kit).

Polymerase chain reaction (PCR) protocol was conducted by mixing 5.0 μL reaction buffer, 1.50 μL of 25 mM $MgCl_2$, 0.50 μL of 10 mM dNTPs, 1.0 μL of 10 μM forward primer 27F 5′-AGAGTTTGATCCTGGCTCAG-3′, 1.0 μL of 10 μM reverse primer1492R 5′-CTACGGCTACCTTGTTACGA-3′, 0.50 μL of taq polymerase, 2.50 μL of DNA sample (45 ng), 13.0 μL of MQ water. 16S rRNA gene sequencing of the purified PCR product was performed by following Sanger method at DNA Solution Ltd., Dhaka, Bangladesh. An amplified sequence was submitted to the National Centre for Biotechnology Information (NCBI), and NCBI BLAST was carried out to distinguish the isolated bacterium.

2.9 Optimization of growth parameter of bacterial culture

Several parameters such as pH (5–11), temperature (35–60 °C), and time (24–96 hours) were optimized. Additionally, the concentration of peptone (0.25–1.5%), yeast extract (0.15–0.90%), and sodium chloride (0.25–1.25%) were optimized. The growth was measured by determining the OD at 600 nm using a colorimeter APEL AP 120 (Japan). The pH, time, temperature, and the specific concentrations of peptone, yeast extract, and sodium chloride at which the growth of the culture was highest were considered the optimum growth parameters.

2.10 Minimum inhibitory concentration (MIC) of chromium

The lowest concentration of chromium that hinders bacterial growth is known as the minimum inhibitory concentration (MIC). Loops containing pure bacterial cultures were streaked on nutrient agar plates that had been spiked with several amounts of chromium (0, 100, 200, 300, 400, 500, 600, 700, 800, 900, and 1000 mg L^{-1}). The plates were incubated for 24 hours at 37 °C. Chromium tolerance was recorded based on the growth of isolates in the media.

2.11 Experimental design

Response surface methodology (RSM) was employed to examine the effect of various independent variables, such as seed volume (A), nutrient source (B), and time (C), on the response variable, which is degradation (Y). According to,[25] the Central Composite Design (CCD) is the standard RSM. It enables estimation of the second-degree polynomial of the relationships between the independent variables as well as the dependent variable. It also provides insights into the interaction between variables and their impact on the dependent variable.[26] Thus, a central composite design with five levels and, three factors, and a quadratic model was chosen to design the experiment. The levels of the selected independent variables used in the experiments are provided in Table 1. Twenty treatments, including six axial points, eight fractional factorial points, and six central points, were randomly performed according to CCD, which is

Table 1 Levels and codes of variables for Central Composite Design (CCD)

	Levels				
Factors	−1.68 (−α)	−1	0	+1	+1.68 (+α)
Seed volume% (v/w)	20	26.08	35	43.92	50
Nutrient source% (w/w)	5	7.02	10	12.97	15
Time (hours)	72	81.72	96	110.27	120

Table 2 Central composite design matrix in coded values, actual and predicted values of the response[a]

	Coded values						Responses	
							Degradation (%)	
Run order	*A*	*B*	*C*	*A*	*B*	*C*	Actual	Predicted
1	0	−α	0	35	5	96	78.00	75.42
2	0	0	0	35	10	96	84.00	89.56
3	+1	−1	+1	43.92	7.02	110.27	92.00	94.07
4	+1	+1	−1	43.92	12.97	81.72	93.00	91.73
5	−1	−1	−1	26.08	7.02	81.72	47.00	49.22
6	−α	0	0	20	10	96	56.00	52.09
7	0	0	−α	35	10	72	74.00	75.42
8	−1	−1	+1	26.08	7.02	110.27	62.00	64.87
9	0	0	0	35	10	96	92.00	89.56
10	0	0	0	35	10	96	88.00	89.56
11	+α	0	0	50	10	96	90.00	91.60
12	+1	+1	+1	43.92	12.97	110.27	93.00	92.39
13	0	0	0	35	10	96	93.00	89.56
14	+1	−1	−1	43.92	7.02	81.72	87.00	85.42
15	0	0	0	35	10	96	86.00	89.56
16	−1	+1	−1	26.08	12.97	81.72	74.00	73.53
17	−1	+1	+1	26.08	12.97	110.27	78.00	81.18
18	0	+α	0	35	15	96	94.00	94.27
19	0	0	0	35	10	96	94.00	89.56
20	0	0	+α	35	10	120	93.00	89.40

[a] *A* = seed volume% (v/w), *B* = nutrient source% (w/w), and *C* = time (hours).

summarized in Table 2. Real levels of independent variables were coded based on eqn (2).

$$x_i = \frac{X_i - X_0}{\Delta X}, i = 1, 2, \ldots, k \quad (2)$$

as a function of an independent variable was represented by the following second-order polynomial equation (eqn (3)).

$$Y = \beta_0 + \sum_{i=1}^{k} \beta_i X_i + \sum_{i=1}^{k} \beta_{ii} X_i^2 + \sum_{i=1}^{k-1} \sum_{j=2}^{k} \beta_{ij} X_i X_j + \varepsilon \quad (3)$$

where Y represents the predicted response, X_i and X_j are the input variables, β_0 is the intercept term, β_i represents the linear effects, β_{ii} is the squared effect, and β_{ij} is the interaction term.[27] The validity of the polynomial equations of the response was confirmed through the application of a statistical test known as ANOVA (Analysis of Variance). Additionally, several determinations of co-efficient such as R^2, predicted R^2, and adjusted R^2, as well as the degree of freedom, were analyzed to verify the reliability of the model. In addition, an analysis was conducted to investigate the effects of independent process variables and their interaction terms on the degradation percentage. This was done by utilizing 3D surface and contour plots. The optimal value for each of the process parameters or independent responses was obtained through the numerical optimization package within the software.

2.12 Experimental process for degradation

Fig. 1 displays the experimental setup of the process. Firstly, shaving dust collected from the tannery area was thoroughly dried in an oven at 100 °C for 30 minutes. Then, 10 mL distilled water per g of chrome shavings and % (w/w) tryptone used as the nutrient source was measured. pH was adjusted with the help of an alkali. The samples in a conical flask were then sterilized by an autoclave machine and cooled to (50–60) °C. Then, % (v/w) bacterial cell suspension (also known as seed) of an initial optical density (OD) of 1.0 was inoculated with a sterilized pipette and run for specific days in a rotary shaker at 150 rpm. The experimental setup depicted in Table 2 was followed, with a seed volume of up to 50% (v/w), a nutrient source of 15% (w/w), and a 120 hour process. Care was taken to inoculate seed volume having the same OD into all the samples. After that, the samples were centrifuged at 10 000 rpm for 20 minutes to separate the microbial cells that settled at the bottom as pellets. The hydrolysate was filtered with filter paper, and the residual weight of shaving dust was noted down after complete drying. The percentage of degradation was then calculated using eqn (4).

$$\%\ \text{of degradation} = \frac{\text{initial weight of shaving dust} - \text{final weight of shaving dust}}{\text{initial weight of shaving dust}} \times 100 \quad (4)$$

where x_i is the dimensionless value of a variable, X_i represents the actual value of the variable, X_0 corresponds to the value of X_i at the center point, and ΔX represents the step change.[26] Experimental data obtained from the CCD were analyzed using the RSM algorithm Design Expert 13.0.5.0 (State Ease, Inc., Minneapolis, MN, USA). The predicted response (degradation)

After that, the hydrolysate was treated with MgO and NaOH at 55 °C on a stirring machine. This process was conducted for two hours to separate the chromium by turning it into insoluble $Cr(OH)_3$. The residual sludge obtained after the degradation was re-suspended in distilled water and subjected to further processing to recover the remaining collagen and chromium.

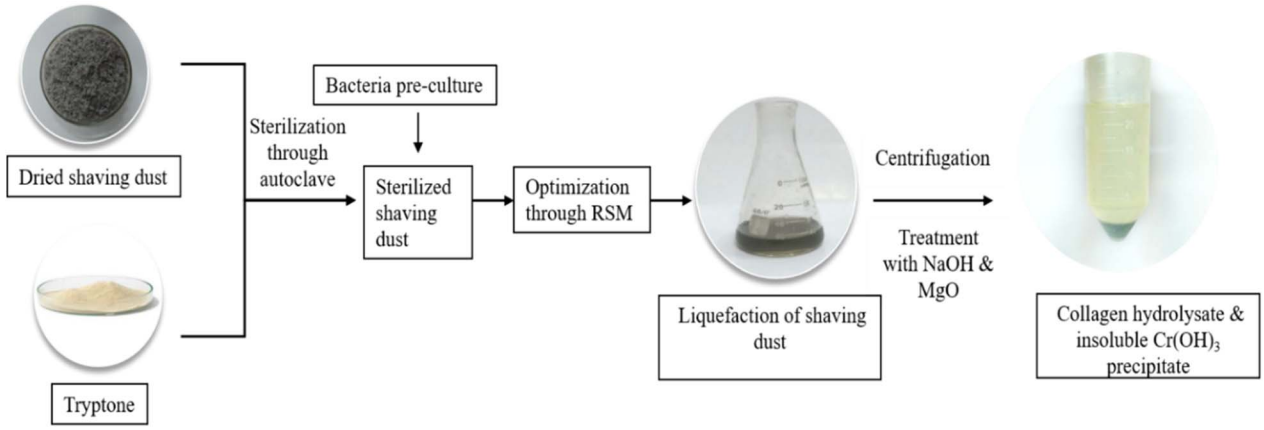

Fig. 1 Flowchart of hydrolysis process through microbial degradation.

After allowing the solution to settle at ambient temperature, the solution was filtered to recover the remaining chrome sludge. The hydrolysate was refrigerated overnight and freeze-dried to obtain a powdered product. This was subsequently employed for characterization purposes.

2.13 Analysis of the collagen hydrolysate and shaving dust

The shaving dust and protein hydrolysate obtained were taken for the following analysis.

2.13.1 Protein content. Bradford's technique was used to measure the protein content. In brief, 100 mg of Coomassie Brilliant Blue G-250, which is the protein reagent, was dissolved in 50 mL of 95% ethanol (C_2H_5OH). Subsequently, 100 mL of 85% phosphoric acid (H_3PO_4) was cautiously added while stirring, and then 1 L of water was added. The solution was filtered and stored at 4 °C. Bovine serum albumin (BSA) (0, 0.0625, 0.125, 0.25, 0.5, and 1 g L^{-1}) was used for generating a standard curve, and absorbance was recorded at 595 nm. Next, 0.1 mL of the collagen solution was taken into test tubes, followed by the addition of 5 mL of protein reagent, and it was left to incubate for 5 minutes. After that, the absorbance at 595 nm was recorded. Protein content in unknown samples was calculated by plotting the absorbance of protein against the equivalent absorbance of a standard curve.[28]

2.13.2 Chromium content. Samples weighing 1.0 g each were treated in a 3 : 1 ratio using 15 mL HCl and 5 mL HNO_3. After that, the sample was heated on a hot plate, and the temperature was progressively raised until the decomposition process was finished and the volume evaporated to roughly 5 mL. Atomic absorption spectroscopy (AAS, PinAAcle 900H, PerkinElmer, USA) was used to evaluate the chromium content of the samples after they had been filtered and diluted with deionized water.[29]

2.13.3 Moisture content. Collagen hydrolysate's moisture content was calculated using ASTM D3790-2012 guidelines. 10 mL of collagen hydrolysate were measured into a crucible, heated to 85 °C for 75 minutes using a heating mantle, and then the samples were brought out and weighed again. This process was carried out again until a steady weight was attained, and the samples' moisture content was determined using the weight loss.[30] The moisture content was measured using eqn (5):

$$\%\ \text{moisture content} = \frac{\text{initial weight with sample} - \text{final weight with sample}}{\text{initial weight with sample}} \times 100 \quad (5)$$

2.13.4 Ash content. The crucibles were numbered, pre-washed with 0.2 N HCl, dried, and stored in a desiccator before their weight was noted down. Then, 1 g of the sample was taken in a crucible and then heated in a muffle furnace at 700 °C for 2 hours. The samples were taken out and cooled in a desiccator, weighed, and the ash content was measured using eqn (6):

$$\%\ \text{ash content} = \frac{\text{weight of the crucible with ash} - \text{weight of the crucible}}{\text{weight of the sample}} \times 100 \quad (6)$$

2.14 Characterizations

2.14.1 UV-vis absorption spectroscopy. UV-visible spectra (T60 UV-visible spectrophotometer, PG Instruments Ltd. England) were measured using the 200–800 nm wavelength range. A plot of absorbance *vs.* wavelength was taken to get the absorption spectra.

2.14.2 Fourier transform infrared spectroscopy (FT-IR). FTIR (Bruker ALPHA II FT-IR Spectrometer, Germany) analysis is used to analyze the existence of various functional groups along with changes in the secondary structure of the sample in the region of 4000–500 cm^{-1} wave numbers at 4 cm^{-1} resolutions.

2.14.3 Thermogravimetric analysis (TGA). Thermal gravimetric analysis (TGA) was conducted using a thermogravimetric analyzer (TGA 8000, PerkinElmer, USA). Approximately 5 mg of the sample was taken in a platinum crucible on the pan of the microbalance, and heating was done from 50 °C to 700 °C with a heating rate of 10 °C min^{-1} under the nitrogen atmosphere at a flow rate of 20 mL min^{-1}.

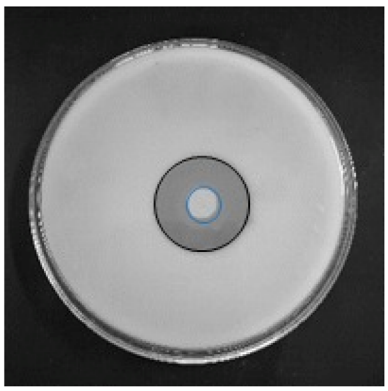

Fig. 2 The growth and zone of proteolytic bacteria in skimmed milk agar after 48 hours.

2.14.4 Scanning electron microscopy (SEM) and elemental analysis. The morphological characterization of the lyophilized collagen hydrolysate was performed using a Scanning Electron Microscope (JSM-7610F, JEOL Ltd. Japan). The sample was affixed to the stage using carbon conductive tape. An Energy Dispersive X-ray spectrometer (EDX) was utilized for the elemental analysis. The method enables the analysis of elemental composition, offering insights into the distribution of particle components. The findings were presented in terms of mass (%).

3 Results and discussion

3.1 Isolation and screening of proteolytic bacterial isolate

From the primary screening process, the bacterial isolate with the highest zone of clearance in the skim milk agar media was selected for secondary screening. It was found that the diameter of the zone of clearance was 14 mm after 24 hours and 28 mm after 48 hours shown in Fig. 2.

The bacterial isolate was then grown in a nutrient agar medium to study its morphological characteristics. The morphological and biochemical results of the selected bacterial isolate are given in Fig. S1 and Tables S1–S3 in the ESI.† After secondary screening, the bacteria's proteolytic activity was found to be 20 U mL^{-1}. The antibiotic susceptivity test for the isolated bacteria was also conducted and is given in Fig. S2 and Table S4.†

3.2 Molecular identification

The genomic DNA of the selected bacterial isolate was extracted and subsequently amplified by polymerase chain reaction (PCR). Gel electrophoresis of the DNA was done and compared with the NEB 100bp DNA ladder. The DNA fragment of the isolated bacterium was around 1500 bp, which means that the mass of the DNA fragment was 45 ng. The DNA was used for the identification of the bacteria. The sequence was uploaded to NCBI GenBank, and Blast result showed that based on the

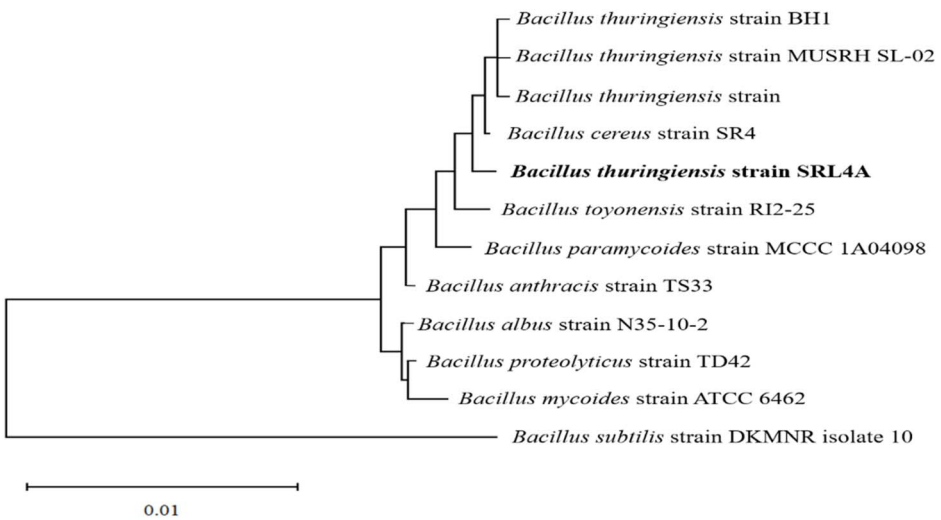

Fig. 3 The phylogenetic tree of *Bacillus thuringiensis* SRL4A.

analysis on NCBI, the 16S rRNA gene sequence of the isolated bacterium had a 99.57% similar percent identity with a maximum score of 2553, the total score of 2553, query cover of 100%, and an *E* value of 0.00 with two bacteria, namely *Bacillus thuringiensis* strain (sequence ID: MK878553.1; length: 1425) and *Bacillus thuringiensis* strain BH1 (sequence ID: KY910253.1; length: 1483).

These results matched with the result obtained from APIWEB™, which was used for the primary identification of the bacteria. So, the isolated bacterium is *Bacillus thuringiensis*, which is closely related to the bacterium *Bacillus cereus* and is a member of the *Bacillus cereus* group. This strain was uploaded to NCBI with the name *Bacillus thuringiensis* SRL4A, and the accession number is PP802975. A phylogenetic tree was constructed using the neighbouring joining method *via* the Mega software (Version 11.0.13) and illustrated in Fig. 3.

3.3 Optimization of growth conditions and culture medium of the bacterium

The optimum parameters for the bacteria were determined by measuring the optical density (OD). The level of light scattering

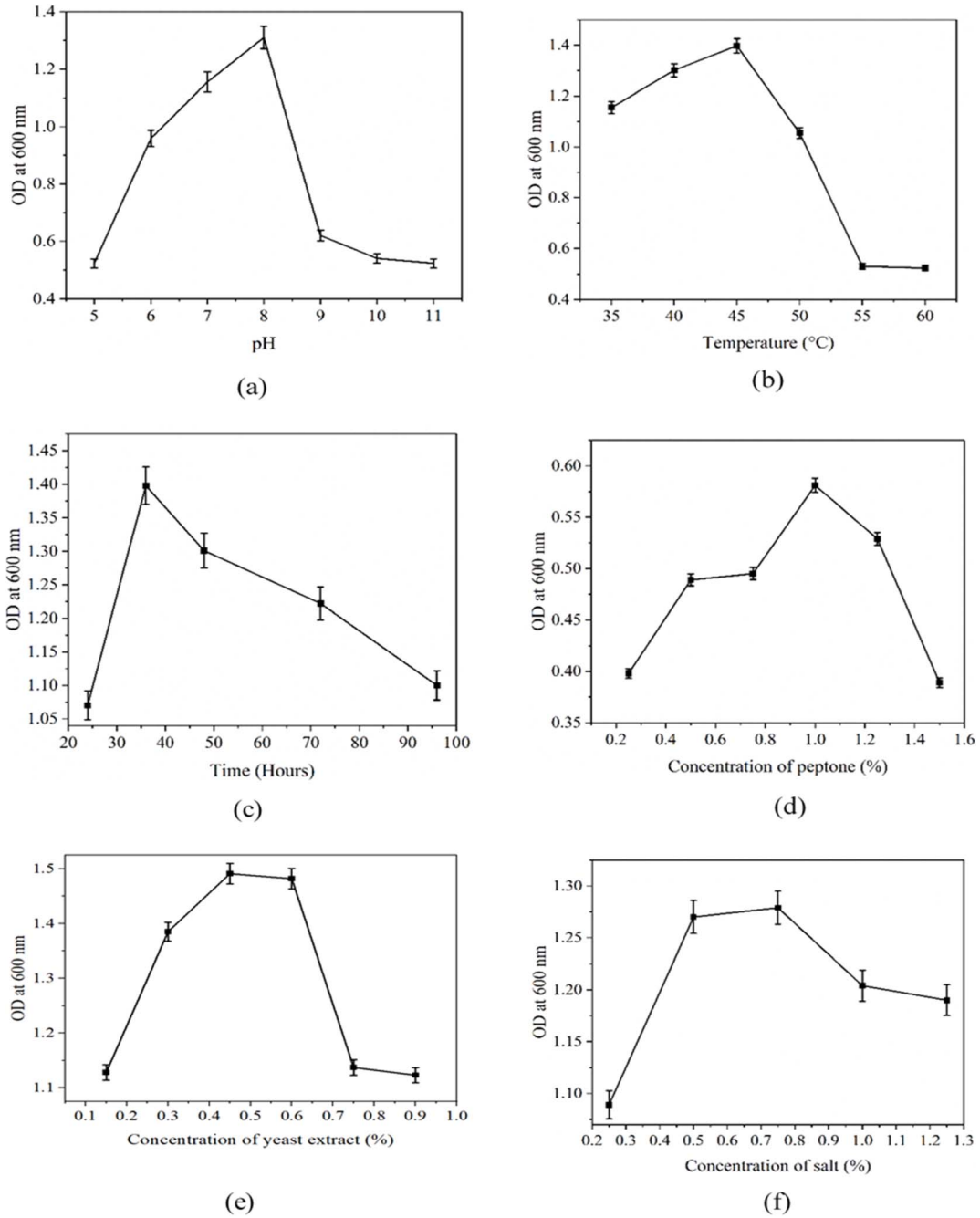

Fig. 4 Optimization of growth condition and culture medium of bacteria. (a) pH, (b) temperature, (c) time, (d) concentration of peptone, (e) concentration of yeast extract, and (f) concentration of salt. The error bar shows for three experimental data.

in a culture is determined by the concentration of bacteria present, with higher concentrations resulting in increased light scattering. The 600 nm wavelength has been selected for bacterial optical density (OD) measurements due to its non-harmful nature to the culture, unlike UV wavelengths. According to the data presented in Fig. 4a, it is evident that the strain SRL4A exhibited the highest bacterial growth at pH 8. The lowest value of OD was observed at pH 5. The growth exhibited a significant reduction under both acidic and alkaline pH conditions. Fig. 4b illustrates the effect of temperature on the growth of the strain. The growth of the bacterium reached its peak at 45 °C, displaying the highest OD of 1.398. However, the growth rate significantly declined as the temperature increased from 45 to 60 °C. In a study conducted by G. G. Khachatourians,[31] it was found that *Bacillus thuringiensis* cells can thrive in temperatures within a range of 10–45 °C. Thus, the degradation process with the bacteria was done at pH 8.00 and a temperature 45 °C. Fig. 4c illustrates that the growth of the bacterium was highest after 36 hours of incubation. The presence of nitrogen sources is crucial for bacteria as it is a fundamental element in various biomolecules such as amino acids, nucleic acids (DNA and RNA), vitamins, and certain coenzymes. It also plays a critical role in the growth and survival of the bacteria. Fig. 4d and e illustrate the growth of the bacterium at varying concentrations of nitrogen source. The optimal condition for maximum growth of the strain SRL4A was at a concentration of 1% peptone. The growth exhibited a gradual decline following an initial increase in concentration from 1%. Similar findings were observed for *Bacillus* spp. by Qadar *et al.* (2009).[32] The optimum yeast extract concentration was 0.45% (Fig. 4e). Khachatourians, (2009)[31] stated that *Bacillus thuringiensis* cells can withstand high levels of NaCl up to 7%. However, in this instance, the bacteria's growth peaked at 0.75% NaCl concentration and progressively declined as the salt concentration increased (Fig. 4f).

3.4 Minimum inhibitory concentration (MIC) of bacteria

The minimum inhibitory concentration represents the lowest chromium concentration that prevents the apparent *in vitro* growth of bacteria. The minimum inhibitory concentration (MIC) of the bacteria for [Cr(III)] salt was determined using the quaternary streaking method on a nutrient agar medium with chrome concentrations ranging from 100 to 1000 mg L^{-1}, as illustrated in Fig. S3 (ESI).† The bacteria exhibited robust growth in media with chromium concentrations up to 700 ppm. The growth rate started to decline steadily at 800, and after 24 hours, there was no more growth when the chromium content in the nutrient agar medium reached 1000 mg L^{-1}.

This suggests that the bacterium is extremely resistant to chromium, as 1000 mg L^{-1} is the minimum inhibitory concentration of bacteria. Similar observations for chromium tolerance of *Bacillus thuringiensis* up to 1000 mg L^{-1} were also reported in the literature.[33]

3.5 Statistical analysis

The response data were analyzed by default without any data transformation in the Design Expert software. Next, the effects for all model terms were calculated, and various statistics including lack of fit, *F*-values, and R^2-values were utilized for comparing the models. Finally, a quadratic model was selected.

The model terms in the equations are determined through a process of eliminating some insignificant variables and their interactions having *p*-values greater than 0.1. Additionally, the terms with the lowest *F*-values were also removed. The summary of ANOVA results for all responses can be found in Table 3. The adequacy of the model was assessed by conducting lack-of-fit *F*-tests. The comparison between the residual error and the pure error is a key aspect of lack of fit. It is preferable to have a small *F* value and a probability greater than 0.1. According to ref. 34, if a model demonstrates a lack of fit, it is not suitable for predicting the response. As shown in Table 3, the lack-of-fit of the model is not statistically significant with a probability of greater than 0.1. This suggests that the model is accurate in statistical terms. The probability value of the model, which was less than 0.0001, suggests that the model used in this study is highly significant. The model *F*-value of 28.01 indicates that the model is statistically significant. There is only a 0.01% chance that

Table 3 ANOVA for reduced quadratic model for response (*Y*): degradation

Source	Sum of squares	*df*	Mean square	*F*-Value	*p*-Value	Remarks
Model	3318.16	6	553.03	28.01	<0.0001	Significant
A-seed volume	1902.29	1	1902.29	96.36	<0.0001	Significant
B-nutrient source	433.11	1	433.11	21.94	0.0004	Significant
C-time	229.25	1	229.25	11.61	0.0047	Significant
AB	162.00	1	162.00	8.21	0.0133	Significant
A^2	541.91	1	541.91	27.45	0.0002	Significant
C^2	83.11	1	83.11	4.21	0.0609	—
Residual	256.64	13	19.74			
Lack of fit	173.14	8	21.64	1.30	0.4041	Not significant
Pure error	83.50	5	16.70			
Cor total	3574.80	19				
Mean	82.40		R^2	0.9282		
Std dev.	4.44		Predicted R^2	0.7986		
C.V.%	5.39		Adjusted R^2	0.8951		
Adequate precision	17.720					

such a large model F-value could occur. Moreover, the models demonstrate an extremely high determination coefficient of 0.9282 (R^2). The R^2-value is a metric that quantifies the extent to which variability in the observed responses can be explained by the experimental variables along with their interactions. A higher R^2-value closer to 1 indicates a stronger predictive ability of the model for the response.[35] Alternatively, lower R^2 values indicate that response variables were not suitable for explaining the variability in behavior.[36] In this study, proximity to unity R^2 demonstrates that the influence of seed volume (A), nutrient source (B), and time (C) on response variables could be adequately described using a quadratic polynomial model. The difference between predicted R^2 and adjusted R^2 should be less than 0.2 for reasonable agreement between the two coefficients. In this case, predicted R^2 and adjusted R^2 values were 0.7986 and 0.8951, respectively, showing a good agreement. The low values of the coefficient of variation (5.39) indicate very good precision and reliability of the experiments.[37] When evaluating the signal-to-noise ratio, it is generally considered desirable to have a ratio greater than 4.[38] This measurement, known as adequate precision, helps assess the quality of the signal in relation to the background noise. The ratio of 17.720 suggests an adequate signal. Thus, this model can be used to navigate the design space.

Furthermore, the residual, which is the variability between the predicted and experimental responses, is employed to assess the accuracy of the model. The residuals are regarded as changes in the model that are not well-fitted.[39] Fig. 5 displays the residual curve for assessing their normal distribution. A straight line is formed by the points on the normal curve, which suggests that the residuals are distributed normally. Predicted *vs.* experimental yield plot, plot of residuals *vs.* run, Cook's distance plot, Box–Cox plot for power transforms, and desirability plot for the degradation of shaving dust are illustrated in Fig. S4 and S5.†

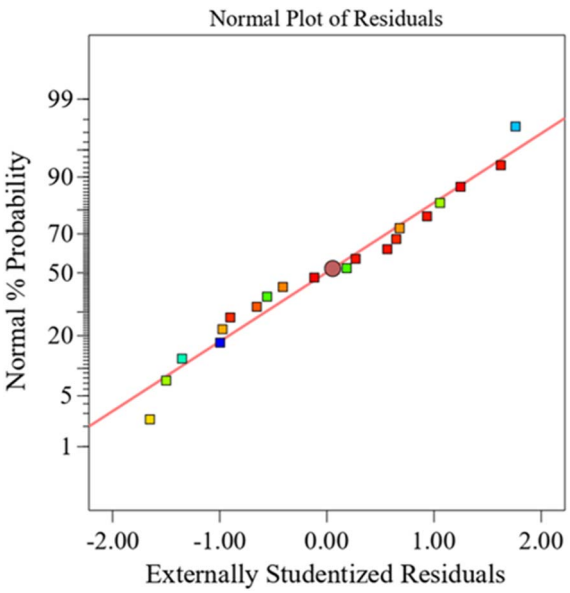

Fig. 5 Normal probability plot for degradation (percent *vs.* residuals).

3.6 Effect of individual process parameters

The microbial degradation of tannery shaving dust was carried out by varying three independent parameters namely bacterial pre-culture (seed) volume, nutrient source, and time. Before microbial degradation, a preliminary pre-treatment of chrome shavings is essential. The stability of collagen is enhanced through the formation of complexes with the carboxyl groups of aspartic and glutamic acid side chains by chromium. Chrome shaving degradation may occur through the disruption of bonds between chrome and protein or the cleavage of peptide bonds. The tightly coiled collagen triple helical structure poses a challenge for enzymatic degradation due to the limited penetration of enzymes into the cross-linked superstructure.[40] To address this issue, chrome shaving dust was autoclaved, which served the dual purpose of sterilization and loosening of the fiber.[13] Additionally, it also made the fiber susceptible to bacterial attack. When bacterial pre-culture is inoculated in the flask, firstly, bacteria attack the peptide bond of loose fibers. They generate bacterial collagenases, which are typically thought of as enzymes that break down helical regions of fibrillary collagen molecules under normal physiological conditions such as pH, temperature, and agitation.[41] They degrade the collagen into simpler compounds and release various substances, including amino acids, and amines.

The bacteria take nutrients from these simpler molecules for rapid growth and start multiplying. As bacterial and enzymatic activities progress, the fibers start to break down further, and the decaying mass may become increasingly liquefied. Based on the data presented in Fig. 6a, it is evident that as the concentration of bacteria increases, the percentage of microbial degradation increases. Prior research also showed that the rate of biodegradation is proportional to the size of the microbe population.[42] Nutrients support the growth and reproduction of microbes, which are essential for breaking down matter.[43] When the concentration of nutrients is increased, there is a corresponding increase in the number of microbes and their metabolic effectiveness. In a previous study, researchers utilized peptone, skimmed milk, soya bean meal, and yeast extract as a nutrient source.[13] This study utilized tryptone as the exclusive nutrient source. The same outcome is seen in Fig. 6b, where an increase in the concentration of tryptone utilized as a nutrient source was accompanied by an increase in the degradation rate. Fig. 6c illustrates the impact of time on

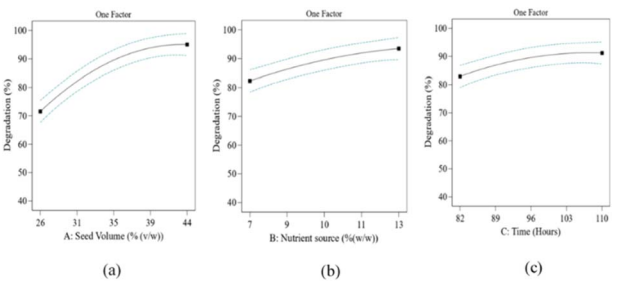

Fig. 6 One-factor plot (a) degradation *vs.* seed volume, (b) degradation *vs.* nutrient source, and (c) degradation *vs.* time.

degradation. Over time, the level of degradation increases. Similar results were also reported in literature.[13] After reaching a seed volume of 35% and a time of 96 hours, any further increase in seed volume and time had minimal impact on the degradation rate. One possible explanation for this phenomenon could be the restricted accessibility of different nutrient sources in the media. After 96 hours, 94% degradation was achieved, leading to a dark green coloration in the supernatant attributed to the presence of Cr^{3+}. These excessive levels of chromium accumulation might also impede the organism's growth and function. From Table 3, it is evident that the seed volume (A) and its squared term (A^2), nutrient source (B), and time (C) have p-values less than 0.05.

This indicates that these parameters play a significant role in the degradation process. Among these, the p-value for seed volume is less than 0.0001 indicating its high level of significance. Additionally, the greater F-value further emphasizes the importance of seed volume as a parameter for determining the maximum degradation rate of chrome shaving dust.

3.7 Interaction effect of process parameters

The effect of the interaction of the process variables (seed volume, nutrient source, and time) was analyzed by 3D surface plots and contour plots using design expert software. The simultaneous impact of two parameters was investigated on the degradation rate. The significance of the parameters was determined using ANOVA. The significance of the interaction between seed volume (A) and time (C), as well as nutrient source (B) and time (C), and B^2, was found to be insignificant with p-values greater than 0.05. As a result, these factors were removed from the model to enhance its accuracy.

They are not presented in the ANOVA table as only significant terms have been considered and mentioned. The regression models made to predict the degradation of tannery shaving dust by *Bacillus thuringiensis* SRL4A for coded and actual variables are presented in eqn (7) and (8), respectively.

$$\begin{aligned}\text{Degradation} = {} & 88.1983 + 11.8022A \\ & + 5.63151B + 4.09714C - 4.5AB \\ & - 6.10185A^2 - 2.38954C^2 \end{aligned} \quad (7)$$

$$\begin{aligned}\text{Degradation} = {} & -266.119 + 8.38967A \\ & + 7.8339B + 2.53999C - 0.169706AB \\ & - 0.0767051A^2 - 0.0117338C^2 \end{aligned} \quad (8)$$

The 3D and contour plots in Fig. 7a depict the coupled effect of seed volume and nutrient source on degradation while both are fixed at their central values, that is, 35 for seed volume and 10 for nutrient source. The diagram explicated the linear effect of both variables. The degradation percentages showed an upward trend as the seed volume and nutrient source increased. After reaching a peak of 94%, increasing one parameter whereas the other held at a constant value, had minimal impact on the yield. The curve section in the 3D plot of Fig. 7a suggests a good interactive influence of these two variables on the degradation rate. Although based on eqn (7) and (8), the interaction of seed volume (A) and nutrient source (B) is negative. It means that the increase of A will reduce the significant effect of B. The coupled impact of BC and AC are also shown in Fig. 7c–f respectively. As the seed volume and time, along with the nutrient source and time, increase, degradation also increases. Nonetheless, the interaction between them does not hold much significance in relation to the response. This can be understood from the flat nature of the 3D plot of AC and BC; which indicates that the coupled effect of these process variables on the degradation rate is minimal.[44] The microbial degradation at different time intervals is illustrated in Fig. S6.†

3.8 Validation of the RSM models

The numerical optimization was executed using the desirability function using the Design Expert software. The selected goals for optimizing seed volume were set at a target of 35%. It was found that beyond this value, increasing the seed volume had minimal impact on degradation. The goals for nutrient source and time were set in the experimental range. The dependent parameter (degradation) was set to a maximum level. Based on the given conditions, a total of 95 solutions were provided. Among them, a total of 90 solutions had a desirability of one. However, the solution selected by the software was considered. The optimum values of the independent process variable for maximum degradation (94.80%) were found to be at seed volume 35% (v/w), nutrient source 12.86% (w/w), and time 101.27 hours. The optimum condition obtained by the software was further validated to check the suitability of the model by conducting an actual experiment at a seed volume of 35%, nutrient source of 12%, and time 101 hours in triplicate. The mean experimental value for degradation was 93.67%. The experimental and predicted results demonstrated a high level of agreement, with an error of only 1.22%. This close correspondence serves to validate the reliability of the developed model.

3.9 Analysis of the collagen hydrolysate and shaving dust

The samples were taken out at different time intervals for the determination of protein content, moisture content, ash content, and chromium content in the collagen hydrolysate. Raw shaving dust was also analysed initially. The results are summarized in Tables 4 and 5.

3.10 Characteristic analysis

3.10.1 UV-vis absorption spectroscopy. The obtained collagen hydrolysate was characterized using UV-vis spectroscopy. It is known that the absorption of protein in the range of (250–350 nm) is due to the protein's triple helical structure and aromatic amino acids. Fig. 8 shows the UV-visible spectra of the prepared collagen hydrolysate. The maximum absorption at 280 nm indicates the presence of amino acids in the hydrolysate.

3.10.2 Fourier transform infrared spectroscopy (FTIR). FTIR of the recovered collagen hydrolysate is shown in Fig. 9. The polypeptide, as well as protein repeat units, results in nine distinct IR absorption bands, specifically amides A, B, and I–VII.

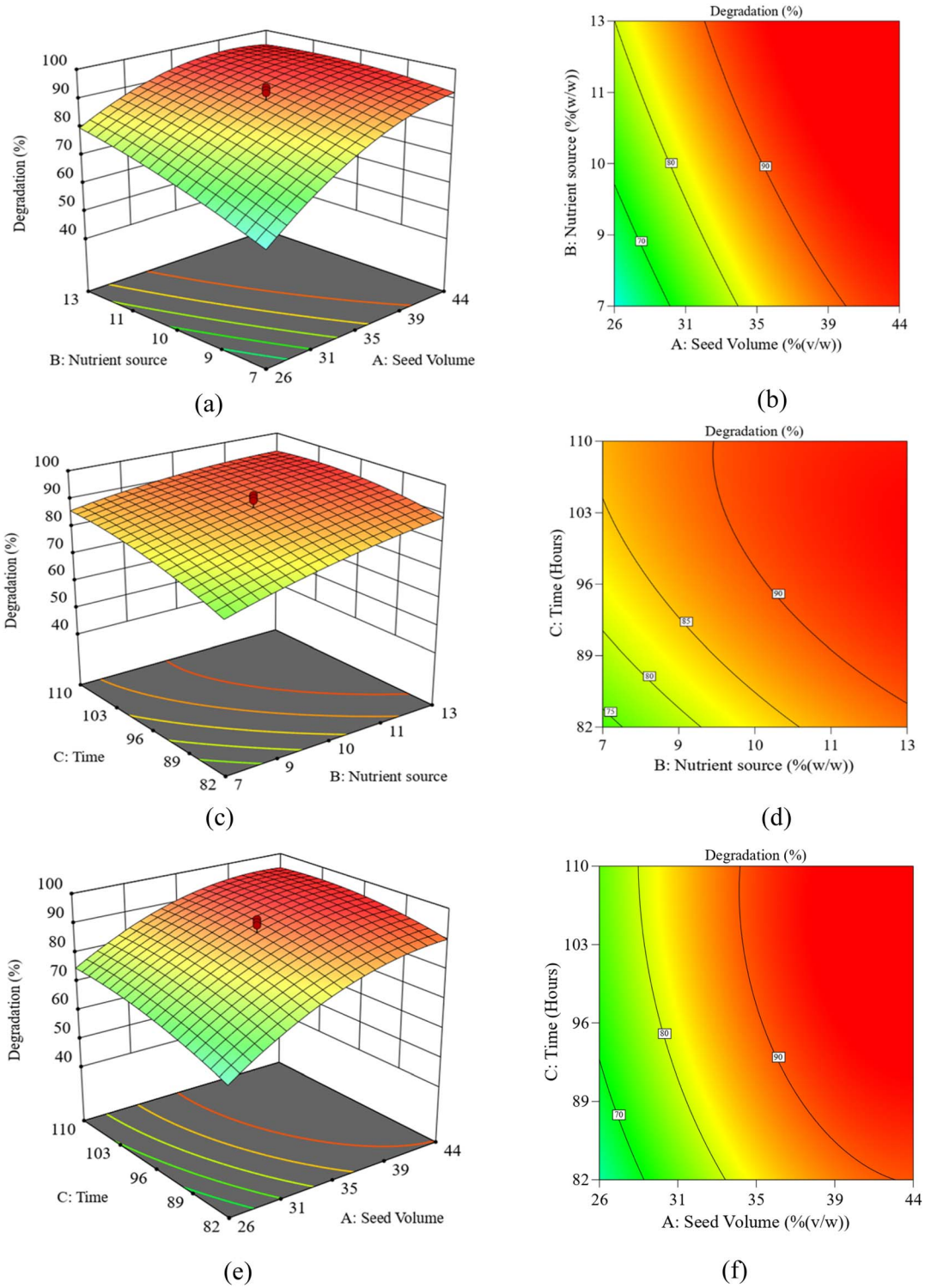

Fig. 7 Response surface plots for effects of seed volume and nutrient source (a), nutrient source and time (c), and seed volume and time (e) on the degradation of chrome tanned shaving dust, and contour plots of interaction between seed volume and nutrient source (b), nutrient source and time (d), and seed volume and time (f) on the degradation of chrome tanned shaving dust.

Two of the most prominent vibrational bands of the protein backbone are the amide I and II bands.[45] One of the most crucial spectral regions for detecting secondary structural components of protein is the amide I band (1700–1600 cm^{-1}), primarily originating from the C=O stretch vibrations of the peptide linkages (around 80%). The FTIR spectrum of pure collagen shows a wide absorption band at 3290 cm^{-1}, which is attributed to the vibration of the hydroxyl (OH) group. The

Table 4 Results of the proximate analysis of the chrome shavings

Name	pH	Protein yield (%)	Total chromium content (ppm)	Total ash (%)	Moisture content (%)
Result	3.45 ± 0.04	88 ± 1.50	171 ± 2.00	13.11 ± 2.1	17.5 ± 1.21

Table 5 Characterization of the recovered collagen hydrolysate

Time (hours)	24	48	72	100
Protein content (mg L^{-1})	471.11 ± 1.13	729.44 ± 1.50	832.77 ± 3.87	979.44 ± 4.88
Total chromium content (ppm)	1.38 ± 0.93	1.80 ± 0.25	2.60 ± 0.58	1.40 ± 0.37
Total ash (%)	9.5 ± 0.40	9.47 ± 1.44	9.94 ± 1.56	9.60 ± 1.82
Moisture content (%)	11.03 ± 1.25	8.75 ± 0.45	10.24 ± 1.95	9.58 ± 2.25

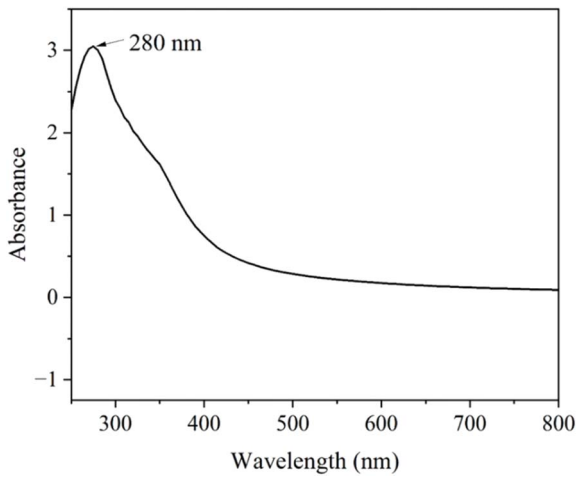

Fig. 8 UV-vis spectra of the recovered collagen hydrolysate.

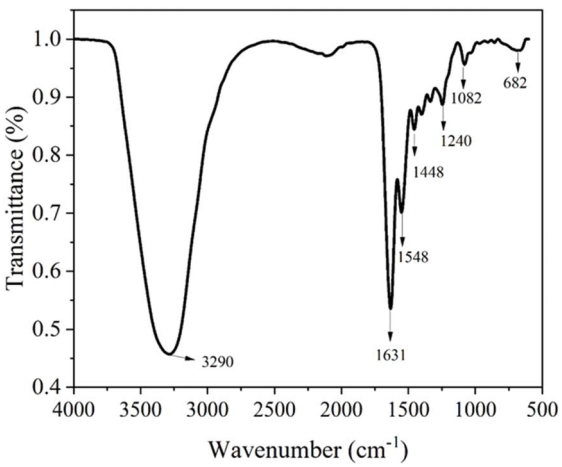

Fig. 9 FTIR spectra of the recovered collagen hydrolysate.

peaks observed in collagen at 1631, 1548, 1240, and 682 cm^{-1} are associated with specific functional groups known as amide I, amide II, amide III, and amide IV respectively. These characteristic peaks proved that the collagen was in hydrolysed form.[46] The bands detected at 1448 and 1082 cm^{-1} are linked to the C–H deformation and C–O stretching of the collagen functional groups.[47]

3.10.3 Thermogravimetric analysis (TGA). The TGA graphs of all the samples are shown in Fig. 10. All the samples showed multi-steps of thermal decomposition. The initial weight loss is due to the removal of residual moisture from the sample. The second stage is related to the peptide degradation in the backbone.[48] As temperature increased, the sample experienced a rapid and substantial weight loss. This loss in weight at the final stage is caused by the degradation of carbonaceous matter and the loss of remaining groups within the samples.[49] The result also showed that the lyophilized collagen powder had higher thermal stability at lower temperatures, but as temperature increases, it becomes more susceptible to degradation.

3.10.4 Scanning electron microscopy (SEM) and elemental analysis. The SEM study of the lyophilized collagen powder is shown in Fig. 11a and S7 in ESI.† The images revealed the

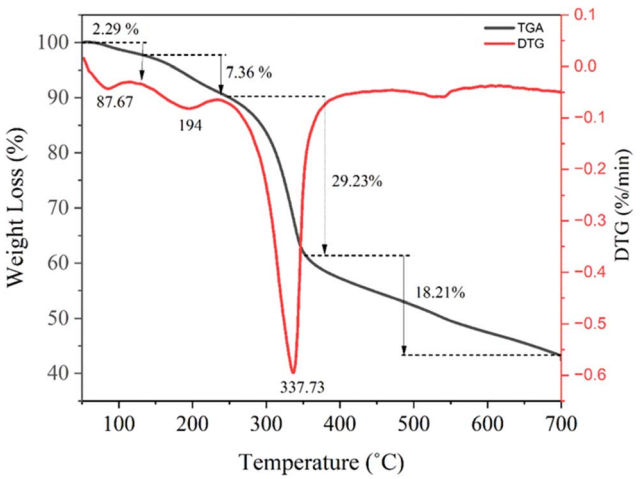

Fig. 10 TGA-DTG curve representing thermal decomposition of recovered collagen hydrolysate.

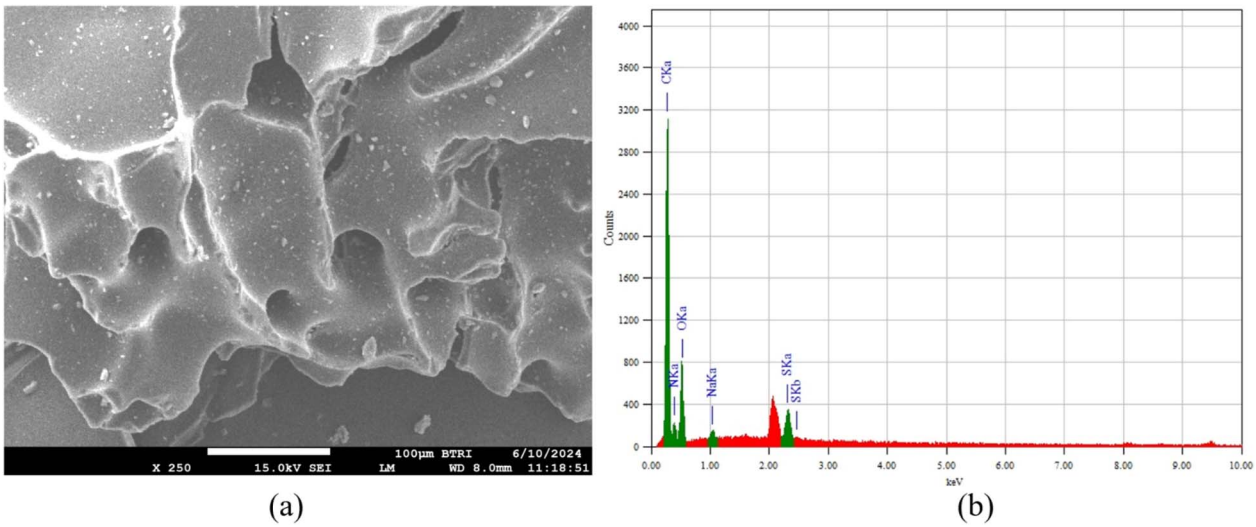

Fig. 11 SEM and EDX analyses of collagen hydrolysate powder recovered from shaving dust *via* microbial degradation.

Table 6 Percentage of different elements determined by Energy Dispersive X-ray analysis (EDX)

Element	Carbon	Nitrogen	Oxygen	Sodium	Sulphur	Total
Mass (%)	50.39	21.52	25.31	0.55	2.23	100.00

presence of irregularly shaped powder particles, densely filled with void spaces or pores. The irregular shape of the sample may be a result of grinding to obtain a fine powder of collagen. In a study conducted by ref. 50, it was observed that protein molecules exhibit significant porosity, characterized by a variety of pore sizes, as a result of their intricate 3D arrangements. The analysis of the lyophilized collagen is presented in Table 6 and Fig. 11b.

The content of carbon, nitrogen, oxygen, sulphur varied from 50.39% to 21.52%, 25.31%, and 2.23% (by mass) respectively. In biological systems, carbon is generally found in higher quantities compared to nitrogen. As per the findings,[51] it has been observed that when the carbon-to-nitrogen ratio within an organic substrate falls between 1 and 15, there is a higher probability of experiencing immediate mineralization and nitrogen release. The sample may biodegrade quickly as a result of this. The data presented in Table 6 indicates that the C/N ratios of the sample fall between 1 and 15. It indicates that the extracted collagens will experience rapid degradation due to the release of nitrogen.

3.11 Comparison with other studies

The extraction percentage of collagen hydrolysate using different methods is shown in Table 7. Due to the cost and complexity of acidic extraction, different alkaline and alkaline-enzymatic treatments are extensively investigated. Nevertheless, the highest yields of collagen hydrolysate through these methods are 60% and 80%, respectively. Table 7 illustrates that although microbial treatment may take longer, it minimizes the use of different chemicals during the extraction process, does not require large energy inputs, and lowers the risk of toxic substances being released into the environment. Most importantly, when compared to traditional physical or chemical treatments, microbial treatments usually result in less sludge; making it easier to handle. Compared to other commonly used procedures, the amount of sludge produced in this study was lower (5–6% on a dry weight basis). Thus, when time, yield, and other processing parameters are compared, it becomes apparent that the microbiological treatment of tannery shaving dust with *Bacillus thuringiensis* is an efficient and sustainable way of extracting collagen hydrolysate from this tannery solid waste.

Table 7 Comparison of collagen hydrolysate extraction yields by various reported methods

		Experimental parameters			
Extraction type	Treatment	Temperature (°C)	Time (hours)	Extraction (%)	Reference
Biocatalytic/enzymatic hydrolysis	Protease, α-amylase & CaO	55	20	80	12
Microbial treatment	*Alcaligenes faecalis*	30	120	90	13
Microbial treatment	*Aspergillus carbonarius*	30	288	97	14
Two-step alkaline-enzymatic hydrolysis	CaO, MgO & 1398 neutral proteinase	80 & 46	6	60	52
Microbial treatment	*Bacillus thuringiensis*	45	101	95	Our study

4 Conclusions

Efforts to detoxify tannery wastes have primarily centered around utilizing enzymes or an amalgam of alkaline and enzymatic hydrolysis. More efficacy in utilizing microbes for the remediation of solid tannery wastes remains needed. The study demonstrates the efficient utilization of bacteria, *Bacillus thuringiensis* strain SRL4A, specifically for the decomposition of shaving dust to recover collagen hydrolysate and chromium. The most favourable growth conditions for the bacteria were a pH of 8, a temperature of 45 °C, and 36 hours of incubation period. The bacterium was resistant to a maximum of 900 ppm of chromium. RSM-based CCD was employed for the optimization of variable parameters for the degradation of shaving dust. The optimum process condition predicted by RSM for maximum degradation (94.80%) was obtained at 35% (v/w) seed volume, 12.86% (w/w), and time 101.27 hours. The experimental conditions were marginally varied and conducted in triplicate at a seed volume of 35%, nutrient source of 12%, and a time of 100 hours. The experimental yield was 93.67% with an error of 1.22%. Additionally, the collagen hydrolysate was characterized by UV-vis spectroscopy, FTIR, TGA, SEM, and EDX. The collagen hydrolysate contained 979.4 ± 4.88 mg L^{-1} of protein and 1.40 ± 0.37 mg L^{-1} of chromium. It suggests that the recovered collagen hydrolysate is safe to be used as fertilizer and as poultry feed. The insoluble chromium that is recovered after precipitation can also be utilized in the re-chroming process by adjusting its basicity with H_2SO_4. Additionally, it can be employed to prepare a variety of ceramic pigments. However, the hydrolysate peptides must undergo a thorough investigation for any contamination from bacterial culture before their use in pharmaceutical applications. Likewise, more studies should be conducted to investigate the potential of collagen hydrolysate as a peptone for the growth of various bacteria. This may be beneficial for cost reduction and material reuse.

Thus, this research study demonstrates that the degradation of chrome shavings studied in this investigation is environmentally friendly and aligns with the principles of a circular economy. The suggested method for managing waste from tanned leather presents a viable and affordable solution for addressing the disposal of this complex waste stream. Additionally, it may aid in material recovery, cost reduction, and land conservation.

Data availability

This manuscript contains all of the data generated or analyzed during this research. The data supporting this article have been included as part of the ESI.†

Author contributions

Abdulla-Al-Mamun M.: conceptualization, methodology, writing – reviewing, supervision, and project administration. Liza S. A.: formal analysis, investigation, data curation, writing – original draft preparation, equal contribution of first authorship. All authors have read and agreed to the publication of the manuscript.

Conflicts of interest

There are no conflicts to declare.

Acknowledgements

The authors extend their sincere appreciation to the Ministry of Science and Technology, Government of the People's Republic of Bangladesh, for the invaluable financial support that significantly contributed to the successful completion of this research project. Additionally, we would like to express our gratitude for the essential analytical and technical support provided by the Centre for Advanced Research in Sciences (CARS), Dhaka University, and the Bangladesh Council for Scientific and Industrial Research (BCSIR). This work was supported by the Ministry of Science and Technology grant under Merit No. 86, Reg. No. 150, Tracking No. 1689011804, provided by the Government of the People's Republic of Bangladesh.

References

1 A. D. Covington and W. R. Wise, *Tanning Chemistry: The Science of Leather*, Royal Society of Chemistry, 2019, DOI: 10.1039/9781839168826.
2 A. A. Belay, Impacts of chromium from tannery effluent and evaluation of alternative treatment options, *J. Environ. Prot.*, 2010, **1**(1), 53, DOI: 10.4236/jep.2010.11007.
3 K. Kolomaznik, M. Mladek, F. Langmaier, D. C. Shelly and M. M. Taylor, Closed loop for chromium in tannery operations, *J. Am. Leather Chem. Assoc.*, 2003, **98**(12), 487–490.
4 S. Tahiri, A. Albizane, A. Messaoudi, M. Azzi, J. Bennazha, S. A. Younssi and M. Bouhria, Thermal behaviour of chrome shavings and of sludges recovered after digestion of tanned solid wastes with calcium hydroxide, *Waste Manag.*, 2007, **27**(1), 89–95, DOI: 10.1016/j.wasman.2005.12.012.
5 S. Saravanabhavan, K. J. Sreeram, J. Raghava Rao and B. Unni Nair, The three pot solution for chromium, tannins and solid wastes: recovery and reuse technique for spent semi-chrome liquor and chrome shavings, *J. Am. Leather Chem. Assoc.*, 2004, **88**(5), 202–207.
6 A. Pati, R. Chaudhary and S. Subramani, A review on management of chrome-tanned leather shavings: a holistic paradigm to combat the environmental issues, *Environ. Sci. Pollut. Res.*, 2014, **21**(19), 11266–11282, DOI: 10.1007/s11356-014-3055-9.
7 H. B. Kerfoot, B. Hagedorn and M. Verwiel, Evaluation of the age of landfill gas methane in landfill gas–natural gas mixtures using co-occurring constituents, *Environ. Sci.: Processes Impacts*, 2013, **15**(6), 1153–1161, DOI: 10.1039/C3EM30971A.
8 A. A. Sasia, P. Sang and A. Onyuka, Recovery of collagen hydrolysate from chrome leather shaving tannery waste

through two-step hydrolysis using magnesium oxide and bating enzyme, *J. Am. Leather Chem. Assoc.*, 2019, **103**(2), 80–84.

9 L. Zhao, S. Mu, W. Wang and H. Gu, Toxicity evaluation of collagen hydrolysates from chrome shavings and their potential use in the preparation of amino acid fertilizer for crop growth, *J. Leather Sci. Eng.*, 2022, **4**, 1–23, DOI: 10.1186/s42825-021-00072-1.

10 A. Rahaman, M. D. Islam and M. M. Raihan, Recovery of chromium from chrome shaving dust, *Eur. J. Acad. Res.*, 2017, **4**(11), 9441–9448.

11 Z. Tian, Y. Wang, H. Wang and K. Zhang, Regeneration of native collagen from hazardous waste: chrome-tanned leather shavings by acid method, *Environ. Sci. Pollut. Res.*, 2020, **27**, 31300–31310, DOI: 10.1007/s11356-020-09183-4.

12 A. Pati, R. Chaudhary and S. Subramani, Biochemical method for extraction and reuse of protein and chromium from chrome leather shavings: a waste to wealth approach, *J. Am. Leather Chem. Assoc.*, 2013, **108**(10), 365–372.

13 C. Shanthi, P. Banerjee, N. C. Babu and G. Rajkumar, Recovery and characterization of protein hydrolysate from chrome shavings by microbial degradation, *J. Am. Leather Chem. Assoc.*, 2013, **108**(6), 231–239.

14 E. A. Katsifas, E. Giannoutsou, M. Lambraki, M. Barla and A. D. Karagouni, Chromium recycling of tannery waste through microbial fermentation, *J. Ind. Microbiol. Biotechnol.*, 2004, **31**(2), 57–62, DOI: 10.1007/s10295-004-0115-z.

15 S. Abinandan and S. Shanthakumar, Evaluation of photosynthetic efficacy and CO_2 removal of microalgae grown in an enriched bicarbonate medium, *3 Biotech*, 2016, **6**, 1–9, DOI: 10.1007/s13205-015-0314-5.

16 K. V. Sandhya, S. Abinandan, N. Vedaraman and K. C. Velappan, Extraction of fleshing oil from waste limed fleshings and biodiesel production, *Waste Manag.*, 2016, **48**, 638–643, DOI: 10.1016/j.wasman.2015.09.033.

17 E. A. Okoroma, H. Garelick, O. O. Abiola and D. Purchase, Identification and characterisation of a Bacillus licheniformis strain with profound keratinase activity for degradation of melanised feather, *Int. Biodeterior. Biodegradation*, 2012, **74**, 54–60, DOI: 10.1016/j.ibiod.2012.07.013.

18 Z. Fang, J. Zhang, B. Liu, G. Du and J. Chen, Biochemical characterization of three keratinolytic enzymes from Stenotrophomonas maltophilia BBE11-1 for biodegrading keratin wastes, *Int. Biodeterior. Biodegradation*, 2013, **82**, 166–172, DOI: 10.1016/j.ibiod.2013.03.008.

19 V. J. Sundar, A. Gnanamani, C. Muralidharan, N. K. Chandrababu and A. B. Mandal, Recovery and utilization of proteinous wastes of leather making: a review, *Rev. Environ. Sci. Biotechnol.*, 2011, **10**(2), 151–163, DOI: 10.1007/s11157-010-9223-6.

20 B. He, Y. Du, H. Xu, J. Ma, C. Cheng and M. Du, Synthesis of Ceramic Pigments with Chromium Content from Leather Waste, *Trans. Indian Ceram. Soc.*, 2021, **80**(2), 103–109, DOI: 10.1080/0371750X.2021.1887766.

21 K. Thirunavukarasu, S. Purushothaman, M. K. Gowthaman, T. Nakajima-Kambe, C. Rose and N. R. Kamini, Utilization of fish meal and fish oil for production of Cryptococcus sp. MTCC 5455 lipase and hydrolysis of polyurethane thereof, *J. Food Technol.*, 2015, **52**, 5772–5780, DOI: 10.1007/s13197-014-1697-8.

22 C. Cupp-Enyard, Sigma's non-specific protease activity assay-casein as a substrate, *J. Vis. Exp.*, 2008, **19**, e899, DOI: 10.3791/899.

23 R. Coico, Gram staining, *Curr. Protoc. Microbiol.*, 2006, 1A–3C, DOI: 10.1002/9780471729259.mca03cs00.

24 M. A. Hussey and A. Zayaitz, *Endospore stain protocol*, Am. Soc. Microbiol., 2007, vol. 8, pp. 1–11.

25 J. P. Wang, Y. Z. Chen, X. W. Ge and H. Q. Yu, Optimization of coagulation-flocculation process for a paper-recycling wastewater treatment using response surface methodology, *Colloids Surf., A*, 2007, **302**(1–3), 204–210, DOI: 10.1016/j.colsurfa.2007.02.023.

26 Z. Zheng, Q. Hu, J. Hao, F. Xu, N. Guo, Y. Sun and D. Liu, Statistical optimization of culture conditions for 1, 3-propanediol by Klebsiella pneumoniae AC 15 via central composite design, *Bioresour. Technol.*, 2008, **99**(5), 1052–1056, DOI: 10.1016/j.biortech.2007.02.038.

27 D. C. Montgomery, *Design and Analysis of Experiments*, John Wiley & Sons, 2017.

28 M. M. Bradford, A rapid and sensitive method for the quantitation of microgram quantities of protein utilizing the principle of protein-dye binding, *Anal. Biochem.*, 1976, **72**(1–2), 248–254, DOI: 10.1016/0003-2697(76)90527-3.

29 F. Idera, O. Omotola, U. J. Paul and A. Adedayo, Evaluation of the effectiveness of different acid digestion on sediments, *IOSR J. Appl. Chem.*, 2014, **7**, 39–47, DOI: 10.9790/5736-071213947.

30 M. I. Ugbaja, A. Young, M. I. Uzochukwu and M. O. Aiyejagbara, Development and characterization of composite films using collagen hydrolysate extracted from chromed leather wastes, *Open Access J. Chem.*, 2018, **2**(3), 14–19, DOI: 10.22259/2637-5834.0203003.

31 G. G. Khachatourians, *Insecticides, Microbial*, ed. M. B., T.-E. M. and T. E. Schaechter, Academic Press, 2009, pp. 95–109, DOI: 10.1016/B978-012373944-5.00124-3.

32 S. A. U. Qadar, E. Shireen, S. Iqbal and A. Anwar, Optimization of protease production from newly isolated strain of Bacillus sp., PCSIR EA-3, *Indian J. Biotechnol.*, 2009.

33 D. S. Ilić, I. Dimkić, H. K. Waisi, P. M. Gkorezis, S. Hamidović, V. Raičević and B. Lalević, Reduction of hexavalent chromium by Bacillus spp. Isolated from heavy metal-polluted soil, *Chem. Ind. Chem. Eng. Q.*, 2019, **25**(3), 247–258, DOI: 10.2298/CICEQ180607003I.

34 S. L. C. Ferreira, R. E. Bruns, E. G. P. da Silva, W. N. L. Dos Santos, C. M. Quintella, J. M. David, J. B. de Andrade, M. C. Breitkreitz, I. C. S. F. Jardim and B. B. Neto, Statistical designs and response surface techniques for the optimization of chromatographic systems, *J. Chromatogr., A*, 2007, **1158**(1–2), 2–14, DOI: 10.1016/j.chroma.2007.03.051.

35 H. L. Liu and Y. R. Chiou, Optimal decolorization efficiency of Reactive Red 239 by UV/TiO_2 photocatalytic process coupled with response surface methodology, *Chem. Eng. J.*, 2005, **112**(1–3), 173–179, DOI: 10.1016/j.cej.2005.07.012.

36 R. H. Myers, D. C. Montgomery and C. M. Anderson-Cook, *Response Surface Methodology: Process and Product Optimization Using Designed Experiments*, John Wiley & Sons, 4th edn, 2016.

37 A. A. L. Zinatizadeh, A. R. Mohamed, A. Z. Abdullah, M. D. Mashitah, M. H Isa and G. D. Najafpour, Process modeling and analysis of palm oil mill effluent treatment in an up-flow anaerobic sludge fixed film bioreactor using response surface methodology (RSM), *Water Res.*, 2006, **40**(17), 3193–3208, DOI: 10.1016/j.watres.2006.07.005.

38 B. K. Körbahti and M. A. Rauf, Response surface methodology (RSM) analysis of photoinduced decoloration of toludine blue, *Chem. Eng. J.*, 2008, **136**(1), 25–30, DOI: 10.1016/j.cej.2007.03.007.

39 S. M. Beck, H. Sabarez, V. Gaukel and K. Knoerzer, Enhancement of convective drying by application of airborne ultrasound–a response surface approach, *Ultrason. Sonochem.*, 2014, **21**(6), 2144–2150, DOI: 10.1016/j.ultsonch.2014.02.013.

40 N. N. Fathima, M. C. Bose, J. R. Rao and B. U. Nair, Stabilization of type I collagen against collagenases (type I) and thermal degradation using iron complex, *J. Inorg. Biochem.*, 2006, **100**(11), DOI: 10.1016/j.jinorgbio.2006.06.014.

41 D. J. Harrington, Bacterial collagenases and collagen-degrading enzymes and their potential role in human disease, *J. Infect. Dis. Immun.*, 1996, **64**(6), 1885–1891, DOI: 10.1128/iai.64.6.1885-1891.1996.

42 N. Hamamura, S. H. Olson, D. M. Ward and W. P. Inskeep, Microbial population dynamics associated with crude-oil biodegradation in diverse soils, *Appl. Environ. Microbiol.*, 2006, **72**(9), 6316–6324, DOI: 10.1128/AEM.01015-06.

43 S. S. Merchant and J. D. Helmann, Elemental economy: microbial strategies for optimizing growth in the face of nutrient limitation, *Adv. Microb. Physiol.*, 2012, **60**, 91–210, DOI: 10.1016/B978-0-12-398264-3.00002-4.

44 S. Singh, J. P. Chakraborty and M. K. Mondal, Pyrolysis of torrefied biomass: optimization of process parameters using response surface methodology, characterization, and comparison of properties of pyrolysis oil from raw biomass, *J. Clean. Prod.*, 2020, **272**, 122517, DOI: 10.1016/j.jclepro.2020.122517.

45 S. Krimm and J. Bandekar, Vibrational spectroscopy and conformation of peptides, polypeptides, and proteins, *Adv. Protein Chem.*, 1986, **38**, 181–364, DOI: 10.1016/S0065-3233(08)60528-8.

46 M. Inan, D. A. Kaya and M. G. Albu, The effect of lavender essential oils on collagen hydrolysate, *Rev. Clim.*, 2013, **64**, 1037–1042.

47 R. Murali, A. Anumary, M. Ashokkumar, P. Thanikaivelan and B. Chandrasekaran, Hybrid biodegradable films from collagenous wastes and natural polymers for biomedical applications, *Waste Biomass Valorization*, 2011, **2**, 323–335, DOI: 10.1007/s12649-011-9072-8.

48 R. Kumar, R. D. Anandjiwala and A. Kumar, Thermal and mechanical properties of mandelic acid-incorporated soy protein films, *J. Therm. Anal. Calorim.*, 2016, **123**, 1273–1279, DOI: 10.1007/s10973-015-5035-9.

49 J. A. Lee, M. J. Yoon, E. S. Lee, D. Y. Lim and K. Y. Kim, Preparation and characterization of cellulose nanofibers (CNFs) from microcrystalline cellulose (MCC) and CNF/polyamide 6 composites, *Macromol. Res.*, 2014, **22**(7), 738–745, DOI: 10.1007/s13233-014-2121-y.

50 S. Abe, H. Tabe, H. Ijiri, K. Yamashita, K. Hirata, K. Atsumi, T. Shimoi, M. Akai, H. Mori, S. Kitagawa and T. Ueno, Crystal Engineering of Self-Assembled Porous Protein Materials in Living Cells, *ACS Nano*, 2017, **11**(3), 2410–2419, DOI: 10.1021/acsnano.6b06099.

51 G. E. Brust, Management strategies for organic vegetable fertility, in *Safety and Practice for Organic Food*, Academic Press, 2019, pp. 193–212, DOI: 10.1016/B978-0-12-812060-6.00009-X.

52 X. H. Qiang and H. Feng, Collagen extracted from chrome shavings using alkali and Enzyme, *2011 International Conference on Remote Sensing, Environment and Transportation Engineering, RSETE 2011 – Proceedings*, 2011, pp. 5810–5813, DOI: 10.1109/RSETE.2011.5965675.